USC–SIPI REPORT #255

Self-Similar Set Identification In The Time-Scale Domain

by

Sam Heidari, George A. Tsihrintzis and Chrysostomos L. Nikias

March 1994

Signal and Image Processing Institute
UNIVERSITY OF SOUTHERN CALIFORNIA
Department of Electrical Engineering-Systems
3740 McClintock Avenue, Room 404
Los Angeles, CA 90089-2564 U.S.A.

Self–Similar Set Identification In The Time–Scale Domain [1]

Sam Heidari, George A. Tsihrintzis, and Chrysostomos L. Nikias

Signal and Image Processing Institute,
EEB400,
University of Southern California,
3740 McClintock Ave., Los Angeles, CA 90089-2564.

Abstract

This paper presents an extended study of the wavelet transform of self–similar signals and its properties. Theorems are presented regarding the properties of the wavelet transform of deterministic self–similar signals and are used to identify and characterize them. The results are extended to applications of interest such as characterization and analysis of real chaotic signals in the presence of additive noise.

[1]This work was supported by the Office of Naval Research under contract No. N-00014-91-J-4021

1 Introduction

Fractal sets (signals) occupy an important place in our everyday life. There are many natural and man made phenomena, such as the structure of natural landscape, turbulence, and fluctuations of the stock market, the nature of which is essentially fractal [1]. Classical Fourier analysis fails to reveal the structure of fractal signals. Therefore, other signal processing methods to identify and characterize fractal sets are of interest.

A known property of fractal sets is their asymptotic *self-similarity* at small scales [1, 2, 3]. The self–similarity property for a deterministic signal $x(t)$ is defined as follows: for all t, t_0, and $h > 0$, $x(t_0 + ht) - x(t_0) = h^{-H}(x(t_0 + t) - x(t_0))$, where H is the *self-similarity parameter.* Because of the self–similarity property of fractal sets, the *wavelet transform* (a mathematical microscope) has been proposed by many authors [4, 5, 6, 7, 8] as a study tool. The wavelet transform allows the representation of a signal in the time–scale domain; therefore, the self–similarity property is preserved by the wavelet transform and its structure is easy to identify.

This paper presents an extended study of the wavelet transform of self–similar signals and its properties. Theorems are presented regarding the properties of the wavelet transform of deterministic self–similar signals and are used to identify and characterize them. These theorems are concerned with: (1) the self–similarity properties of the wavelet transform of these signals and (2) the Fourier analysis of the wavelet transform of self–similar signals. It is shown that the Fourier transform of the wavelet transform of a self–similar signal is proportional to the wavelet transform of the signal. This fact, along with the known fact that the wavelet transform of a self–similar signal is itself self–similar, is used in the analysis of self–similar signals in the presence of noise.

Another application of interest is in the identification of chaotic signals embedded in noise. The attractors of chaotic signals have fractal properties. The existing methods of characterizing

chaotic signals (e.g. Fractal Dimension [1, 2, 3, 9, 10]) have very poor performance when the signals are embedded in noise [11, 12, 13, 14, 15]. In the presence of additive noise, each member of the attractor set is relocated in the phase space while maintaining its value. For example, in Fig. (1) the attractor of the Henon map is presented and in Fig. (2) the attractor of the Henon map in the presence of additive white Gaussian noise is presented. If each dark mark represents membership in the fractal set, there are the same number of members in both figures, but the members of Fig. (2) are displaced. The displacements are directly related to the statistical properties of the additive noise. In the one–dimensional case, the displaced set (signal, $\hat{x}(t)$) and the original set (signal, $x(t)$) are linearly related: $\hat{x}(t) = Ax(t)$. The matrix A is a random permutation matrix and its statistical properties are related to the statistical properties of the additive noise. The advantage in using the wavelet transform to identify randomly moved fractal sets lies in the fact the wavelet transform at coarser scales, where it is less contaminated by noise, suffices to identify and characterize the fractal set. Therefore, we may obtain an estimate of the value of the self–similarity parameter H and subsequently of the fractal dimension of the signal, using information at coarser scales of the wavelet transform only.

The paper is organized as follows: Section 2 is a brief review of the theory of wavelet transforms. In section 3, we present several new theorems concerning the wavelet transform of self–similar sets and the use of these theorems in the development of an algorithm for characterization of fractal sets. In section 4, simulation results are presented for various test cases of fractal sets embedded in noise. Finally, in section 5, we summarize the key findings of the paper and suggest possible avenues of future research.

2 Wavelet transforms

The Wavelet Transform is the decomposition of a signal into a set of real basis functions in the time–scale domain [4, 16]. These functions are obtained by dilation and translation of the same *wavelet function*, $\psi(t)$

$$\psi_{a,b}(t) = |a|^{-\frac{1}{2}}\psi\left(\frac{t-b}{a}\right). \tag{1}$$

It is assumed that $\psi \in L^2(\mathcal{R})$ satisfies the *admissibility condition*:

$$C_\psi = 2\pi \int_{-\infty}^{\infty} |\omega|^{-1}|\Psi(\omega)|^2\, d\omega < \infty, \tag{2}$$

where $\Psi(\omega)$ is the Fourier transform of $\psi(t)$. Also assuming $\psi \in L^1(\mathcal{R})$, C_ψ is finite only if $\Psi(0) = \int_{-\infty}^{\infty} \psi(t)dt = 0$.

The Continuous Wavelet Transform (CWT) with respect to the wavelet function $\psi(t)$ is then defined as

$$WT_x^\psi(a,b) = \int_{-\infty}^{\infty} x(t)\psi_{a,b}(t)\, dt. \tag{3}$$

The CWT can be inverted to give

$$x(t) = C_\psi^{-1} \int_{-\infty}^{\infty}\int_{-\infty}^{\infty} WT_x^\psi(a,b)\psi_{a,b}(t)\, \frac{da\, db}{a^2}. \tag{4}$$

Since the CWT is a redundant representation of $x(t)$ and it is not possible to be implemented on a digital computer, the Discrete Wavelet Transform (DWT) has been introduced. The basis functions, $\psi_{m,n}(t)$, of the DWT are defined as $\psi_{a,b}(t)$ for $a = a_0^m$ and $b = nb_0a_0^m$, where $m, n \in \mathcal{Z}$

and $a_0 > 1$, $b_0 > 0$ are fixed and depend on ψ. The discrete wavelet functions are then given as

$$\psi_{m,n}(t) = a_0^{-\frac{m}{2}} \psi\left(\frac{t - nb_0 a_0^m}{a_0^m}\right) = a_0^{-\frac{m}{2}} \psi(a_0^{-m}t - nb_0) \tag{5}$$

and the DWT is expressed as

$$b_n^{-m} = \int_{-\infty}^{\infty} x(t)\psi_{m,n}(t)dt \tag{6}$$

The problem is to choose the values of a_0 and b_0 such that it is possible to reconstruct the signal $x(t)$ from its DWT, $c_{m,n}$, in an optimum way. This is a difficult problem since, as the values of a_0 and b_0 approach 1 and 0, respectively, the DWT becomes redundant; on the other hand, if a_0 and b_0 are too large then information is lost and accurate reconstruction of $x(t)$ is not possible. It has been shown [17, 18] that if $\psi(t)$ meets certain conditions, then the set $\{\psi_{m,n}(t) = 2^{-\frac{m}{2}}\psi(2^{-m}t - n)|m, n \in \mathcal{Z}\}$, (i.e., $a_0 = 2, b_0 = 1$) will form an *orthonormal* basis in $L^2(\mathcal{R})$. It is necessary that we state some of these conditions, but in preparation, we need to introduce the *scaling function* $\phi(t)$ satisfying the following equations:

$$\phi(t) = \sqrt{2}\sum_n h(n)\phi(2t - n) \tag{7}$$

$$\sum_n \phi(t - n) = 1 \tag{8}$$

$$\int_{-\infty}^{\infty} \phi(t)dt = 1. \tag{9}$$

The scaling coefficients are defined as,

$$a_n^{-m} = \int_{-\infty}^{\infty} x(t)\phi_{m,n}(t)dt. \tag{10}$$

In the above, $h(n)$ is a complex–valued, absolutely summable sequence, the Fourier transform

$H(\omega)$ of which satisfies:

$$|H(\omega)|^2 + |H(\omega + \pi)|^2 = 1 \tag{11}$$

for all $\omega \in \mathcal{R}$ and

$$H(0) = 1. \tag{12}$$

To proceed, the *wavelet function* $\psi(t)$ is related to the scaling function $\phi(t)$ as follows

$$\psi(t) = 2\sum_n g(n)\phi(2t - n) \tag{13}$$

where $g(n) = (-1)^{1-n}\overline{h}(1 - n)$ with the overbar denoting the complex conjugate. Its Fourier transform, $G(\omega)$, vanishes at $\omega = 0$. In [18], it is proved that ψ and ϕ are square integrable and their $L^2(\mathcal{R})$ norms are equal to each other and are less than one. *It is also proved [19] that the necessary and sufficient condition for the set* $\{\psi_{m,n}(t) = 2^{-\frac{m}{2}}\psi(2^{-m}t - n)|m, n \in \mathcal{Z}\}$ *to form an orthonormal basis in* $L^2(\mathcal{R})$ *is that the set* $\{\phi(t - n)|n \in \mathcal{Z}\}$ *be orthonormal* or, equivalently, that

$$\sum_n |\Phi(\omega - 2\pi k)|^2 = 1 \tag{14}$$

where $\Phi(\omega)$ is the Fourier transform of $\phi(t)$.

It is necessary to note that not all the $h(n)$ satisfying conditions (11) and (12) will produce orthonormal bases. Next we would like to define some of the wavelet functions that are used often and satisfy the orthonormality property.

2.0.1 Haar Wavelets

The Haar wavelets were introduced by A. Haar (1910) [20] and correspond to the scaling function

$$\phi(t) = \begin{cases} 1 & 0 \leq t \leq 1 \\ 0 & \text{otherwise.} \end{cases} \tag{15}$$

Therefore, the Haar wavelet function (Fig. 3) is

$$\psi(t) = \begin{cases} 1 & 0 \leq t < \frac{1}{2} \\ -1 & \frac{1}{2} \leq t < 1 \\ 0 & \text{otherwise} \end{cases} \tag{16}$$

The set $\{\psi_{m,n}(t) = 2^{-m/2}\psi(2^m t - n) | m, n \in \mathcal{Z}\}$ is, indeed, an orthonormal basis in $L^2(\mathcal{R})$.

2.0.2 Daubechies Wavelets

The Daubechies wavelets are based on the approach that the conditions (7), (8), and (11) be satisfied [17, 21]. Therefore, $h(n)$ is expressed as:

$$h(0) = \frac{c(c-1)}{(c^2+1)\sqrt{2}} \tag{17}$$

$$h(1) = \frac{(1-c)}{(c^2+1)\sqrt{2}} \tag{18}$$

$$h(2) = \frac{(c+1)}{(c^2+1)\sqrt{2}} \tag{19}$$

$$h(3) = \frac{c(c+1)}{(c^2+1)\sqrt{2}}, \tag{20}$$

where c is a real number. The scaling function $\phi(t)$ is found at the limit of the recursion

$$\phi_k(t) = \sqrt{2}\sum_n h(n)\phi_{k-1}(2t-n) \tag{21}$$

where $\phi_0(t) = \chi_{[0,1)}(t)$. The above sequence converges for $c = \pm 1/\sqrt{3}$. The wavelet function $\psi(t)$ (Fig. 4) may be constructed from $\phi(t)$ using Eq.(13) [$\psi(t) = 2\sum_n g(n)\phi(2t-n)$]. It is shown that the set $\{\psi_{m,n}(t) = 2^{-m/2}\psi(2^m t - n) | m, n \in \mathcal{Z}\}$ constitutes an orthonormal basis of $L^2(\mathcal{R})$ [21]. The above wavelets (Haar and Daubechies) are very popular and each one is better suited for different application. The results of the following section are, however, independent of the choice of wavelet function. The Haar wavelet is utilized in the simulations because of its simplicity.

3 Self–similar set identification in the time–scale domain

Using the following theorems, the wavelet transform is utilized to identify and characterize self–similar sets.

Theorem 1: *The continuous wavelet transform of a self-similar signal, $x(t)$, is itself self-similar, satisfying $WT(ha, t_0 + hb) = h^{-H+1/2}WT(a, t_0 + b)$* [6, 8]

Proof: The wavelet transform is defined as,

$$WT_x^{\psi}(a,b) = \int_{-\infty}^{\infty} |a|^{-1/2}\psi\left(\frac{t-b}{a}\right)x(t)\ dt \tag{22}$$

$$WT_x^{\psi}(ha, t_0 + hb) = \int_{-\infty}^{\infty} |ha|^{-1/2}\psi\left(\frac{t-t_0-hb}{ha}\right)x(t)\ dt. \tag{23}$$

Substitute ζ for $\frac{t-t_0-hb}{ha}$

$$\begin{aligned} WT_x^{\psi}(ha, t_0+hb) &= \int_{-\infty}^{\infty} |ha|^{1/2}\psi(\zeta)x(ha\zeta+t_0+hb)\ dt \\ &= \int_{-\infty}^{\infty} |ha|^{1/2}\psi(\zeta)x(h(a\zeta+b)+t_0)\ d\zeta \\ &= \int_{-\infty}^{\infty} |ha|^{1/2}\psi(\zeta)(h^{-H}(x(a\zeta+b+t_0)-x(t_0))+x(t_0))\ d\zeta \end{aligned} \tag{24}$$

But, from section 2, we know that $\Psi(0) = \int_{-\infty}^{\infty} \psi(t)dt = 0$, therefore:

$$WT_x^{\psi}(ha, t_0+hb) = \int_{-\infty}^{\infty} |ha|^{1/2}\psi(\zeta)h^{-H}x(a\zeta+b+t_0)d\zeta \tag{25}$$

setting $t = a\zeta + b + t_0$, we get

$$WT_x^{\psi}(ha, t_0+hb) = \int_{-\infty}^{\infty} |ha^{-1}|^{1/2}\psi\left(\frac{t-b-t_0}{a}\right)h^{-H}x(t)dt = h^{-H+1/2}WT_x^{\psi}(a, t_0+b), \tag{26}$$

which proves the theorem.

Q.E.D

Corollary 1: *If $WT(a,b)$ is the wavelet transform of a self-similar signal, then* $WT(ha,b) = h^{-H+1/2}WT(a,b)$.

Proof: Similar to the proof of theorem 1.

The above theorem (1) is extended to the discrete wavelet transform case via sampling of a and b at 2^m and $2^m n$, respectively, since the Discrete Wavelet Transform is defined as $b_n^m = WT(2^m, 2^m n)$. If $h = 2^L$, where L is an integer, then from theorem (1) we have $b_n^{m+L} = 2^{L(-H+1/2)}b_n^m$.

Theorem 2: *Given the scaling coefficients a_n^{-m} of the Discrete Wavelet Transform of a self-similar signal $x(t)$*

$$a_n^{-m} = \int_{-\infty}^{\infty} 2^{-m/2}\phi(2^{-m}t - n)x(t)\ dt \tag{27}$$

and its Discrete Fourier Transform (DFT) $a_n(k)$ with respect to the variable m

$$a_n(k) = \sum_{m=0}^{N-1} a_n^{-m-1} \exp(-j2\pi k\frac{m}{N}) \tag{28}$$

then there exist scalars α_k and β_k depending on k, such that

$$a_n(k) = a_n^{-1}\beta_k - \alpha_k \tag{29}$$

where a_n^{-1} is the scaling coefficient at scale $m = -1$.

Proof: $a_n(k)$ is expressed as:

$$a_n(k) = \sum_m \int_{-\infty}^{\infty} 2^{-(m+1)/2}\phi(2^{-m-1}t - n)x(t)\ dt \exp(-j2\pi k\frac{m}{N}) \tag{30}$$

or, after the change of variable $\zeta = 2^{-m}t$

$$a_n(k) = \sum_m \int_{-\infty}^{\infty} 2^{(m-1)/2}\phi(2^{-1}\zeta - n)x(2^m\zeta)\ d\zeta \exp(-j2\pi k\frac{m}{N}). \tag{31}$$

Using the definition of self-similarity Eq.(31) may be expressed as

$$a_n(k) = \sum_m 2^{m/2} \exp\left(\frac{-j2\pi k}{N}m\right) \int_{-\infty}^{\infty} 2^{-1/2}\phi(2^{-1}\zeta - n)(2^{-mH}(x(\zeta) + x(0)) - x(0))\ d\zeta \tag{32}$$

which after some simple manipulations is brought to the final form

$$a_n(k) = a_n^{-1}\beta_k + \alpha_k. \tag{33}$$

The scalars α_k and β_k have been defined as

$$\beta_k = \sum_m 2^{\frac{m}{2}-mH} \exp\left(\frac{-j2\pi k}{N}m\right) \tag{34}$$

and

$$\alpha_k = \left(\int_{-\infty}^{\infty} 2^{-1/2}\phi(2^{-1}\zeta - n)\ d\zeta\right) \sum_m 2^{\frac{m}{2}} \exp\left(\frac{j2\pi k}{N}m\right)\left(2^{-mH}x(0) - x(0)\right). \tag{35}$$

Using the relation (9), α_k is seem to equal,

$$\alpha_k = x(0) \sum_m 2^{\frac{m}{2}} \exp\left(\frac{-j2\pi k}{N}m\right)\left(2^{-mH} - 1\right). \tag{36}$$

Q.E.D

Theorem 3: *Given the Discrete Wavelet Transform, b_n^m of a self-similar signal $x(t)$*

$$b_n^{-m} = \int_{-\infty}^{\infty} 2^{-m/2}\psi(2^{-m}t - n)x(t)\ dt \tag{37}$$

and its Discrete Fourier Transform (DFT) of b_n^m with respect to the variable m

$$b_n(k) = \sum_m b_n^{-m-1} \exp(-j2\pi k\frac{m}{N}) \tag{38}$$

then there exist scalars β_k, depending onk, such that

$$b_n(k) = b_n^{-1}\beta_k, \tag{39}$$

where b_n^{-1} is the DWT at scale $m = -1$.

Proof: Similar to the proof of theorem 2, but with use of the fact $\int \psi(t-n)dt = 0$. Also note that β_k is equal to β_k defined on theorem 2.

The above theorems (1,2, and 3) will be utilized to identify and characterize self–similar signals by estimating the self–similarity parameter H. Assuming the self–similarity property not to hold for all h, the above theorems will still be valid. For computer simulation purposes, the Cantor sets are consider. It is interesting to note that the Cantor set, according to the definition, is self–similar only for $h = L^m$, where L and m are positive integers. Using the definition of the discrete wavelet function: $\psi_{m,n}(t) = a_0^{-m/2}\psi(a_0^{-m}t - nb_0)$ for $b_0 = 1$ and $a_0 = L$, we show that results are still valid. The value of H may be estimated using corollary 1 or any of the theorems stated above. For a randomly moved self–similar set, one may weight the estimate of coarser scales more. One estimate of H is given as

$$\hat{H} = \mathcal{E}\left\{\frac{1}{2} - \log_h\left(\frac{WT(h^{-L-1}, h^{-L-1}n)}{WT(h^{-L}, h^{-L}n)}\right)\right\} \tag{40}$$

where $\mathcal{E}\{.\}$ is the ensemble average.

4 Simulation results

In this section the wavelet transform of various one–dimensional multifractal signals and their randomly moved versions are presented and compared. Fig.(5) is a self–similar signal, $x(t)$, and

Fig.(6) is the same signal but randomly moved in time, $\hat{x}(t)$. Note that $H = 0$ and $x(t)$ is self–similar for $h = 4^m$, where m is an integer. Fig(7) presents the difference between signals illustrated in Fig. (5) and Fig.(6). In Figs. (8) and (9) respectively the Haar DWT of the signals $x(t)$ and $\hat{x}(t)$ are presented and the self similarity of $x(t)$ is revealed. The Haar wavelet transform was utilized for simplicity.

Figs. (10) and (11) show the auto–correlation of the DWT b_n^m for different m's. Figs. (12) and (13) show the Power Spectral Density of the DWT. Figs. (8) – (13) reveal that the coarser scales of $\hat{x}(t)$ still contains the self–similarity information. In Figs. (14) and (15) the DFT of the wavelet transform $\sum_m b_n^m \exp(j2\pi mk/N)$ is presented.

In the following table, the estimated values of self–similarity parameter H of $x(t)$, $\hat{x}(t)$, and $x(t)$ with additive white Gaussian noise are shown,

m	H of $x(t)$	H of $\hat{x}(t)$	H of $x(t) + n(t)$ for $30dB$ SNR
-1	0	-1.5001	-0.3373 + 0.9596 i
-2	0	-0.5963	-0.3766 + 0.7998 i
-3	0	0.3219	-0.2831 + 0.7554 i
-4	0	0.0060	-0.0026

5 Conclusion

In this report we demonstrated that wavelet transform is a promising tool for multifractal analysis. It was shown that the DFT of the DWT of a self–similar signal is proportional to the DWT of the signal. The results can easily be extended to the continuous wavelet transform case. The theorems stated in this report can be utilized to develop characterization and identification algorithms for self–similar sets. It was shown that if the fractal set is moved in the space, the information in the coarser scales is preserved and may be utilized to characterize the set or to

recover the finer scales. A particular method of estimating the self–similar parameter H was proposed. However, its statistical properties need to be studied further. Since the attractor of a chaotic system in the phase space domain is a high–dimensional image, the theory must be extended to higher–dimensions too.

References

[1] B. B. Mandelbrot, *The Fractal Geometry of Nature.* New York: Freeman, 1982.

[2] K. J. Falconer, *The Geometry of Fractal Sets.* Cambridge: Cambridge University Press, 1986.

[3] H. O. Peitgen, H. Jurgens, and D. Saupe, *Chaos and Fractals, new frontiers of science.* New York: Springer-Verlag, 1992.

[4] Y. Meyer, *Wavelets Algorithms and Applications.* Philadelphia, Penn: SIAM, 1993.

[5] G. W. Wornell, "Wavelet-based representation for the $1/f$ family of fractal processes," *Proceeding of the IEEE*, vol. 81, pp. 1428–1450, 1993.

[6] A. Arneodo and G. Grasseau, "The wavelet transform of multifractals," *Physical Review Letters*, vol. 61, pp. 2281–2284, 1990.

[7] E. Bacry, J. F. Muzy, and A. Arneodo, "Singularity spectrum of fractal signals from wavelet analysis: Exact results," *Journal of Statistical Physics*, vol. 70, pp. 634–674, 1993.

[8] M. Holschneider, "On the wavelet transform of fractal objects," *Journal of Statistical Physics*, vol. 50, pp. 963–993, 1988.

[9] P. Grassberger and I. Procaccia, "Characterization of strange attractors," *Physical Review Letters*, vol. 50, pp. 346–349, 1983.

[10] T. S. Packard and L. O. Chua, "Chaos: A tutorial for engineers," *Proceedings of the IEEE*, vol. 75, pp. 982–1008, 1987.

[11] S. Heidari and C. L. Nikias, "Characterizing chaotic attractors using fourth–order off–diagonal cumulant slices," *Asilomar Conference on Signals, Systems and Computers*, 1993.

[12] A. Passamante, T. Hediger, and M. Gollub, "Fractal dimension and local intrinsic dimension," *Physical Review A*, vol. 39, p. 3640, 1989.

[13] A. Passamante and M. E. Farrell, "Characterizing attractors using local intrinsic dimension via higher-order statistics," *Physical Review A*, vol. 43, p. 5268, 1990.

[14] P. Flandrin and O. Michel, "Higher-order within chaos," *IEEE Signal Processing Workshop on Higher-Order Statistics*, p. 295, 1993.

[15] A. M. Albano, J. Muench, C. Schwartz, A. I. Mees, and P. E. Rapp, "Singular-value decomposition and the Grassberger-Procaccia algorithm," *Phys. Rev. A*, vol. 38, p. 3017, 1980.

[16] I. Daubechies, *Ten Lectures on Wavelets.* Philadelphia, Penn: SIAM, 1992.

[17] I. Daubechies. "The wavelet transform, time-frequency localization and signal analysis," *IEEE Trans. on Info. Theory*, vol. 36, pp. 961–1005, 1990.

[18] W. M. Lawton, "Tight frames of compactly supported affine wavelets," *J. Math. Phys.*, vol. 31, pp. 1898–1901, 1990.

[19] W. M. Lawton, "Necessary and sufficient conditions for constructing orthonormal wavelet bases," *J. Math. Phys.*, vol. 32, pp. 57–61, 1991.

[20] A. Haar, "Zur theorie der orthogonalen funktion-systeme," *Math. Ann.*, vol. 69, pp. 331–371, 1910.

[21] C. K. Chui, *Wavelets: A Tutorial in Theory and Applications, Vol. 2.* San Diego, CA: Academic Press, 1992.

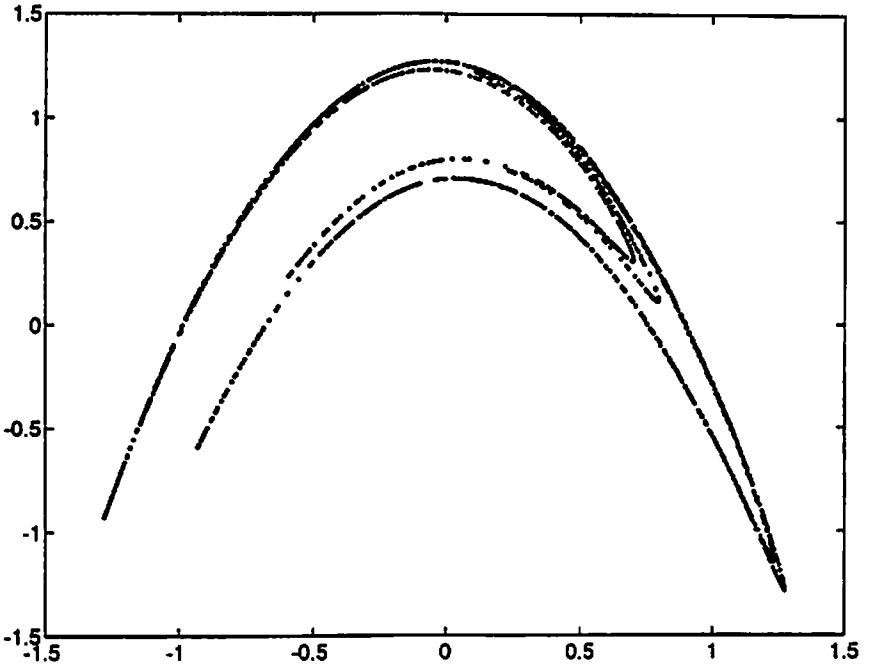

Figure 1: The attractor of the Henon map.

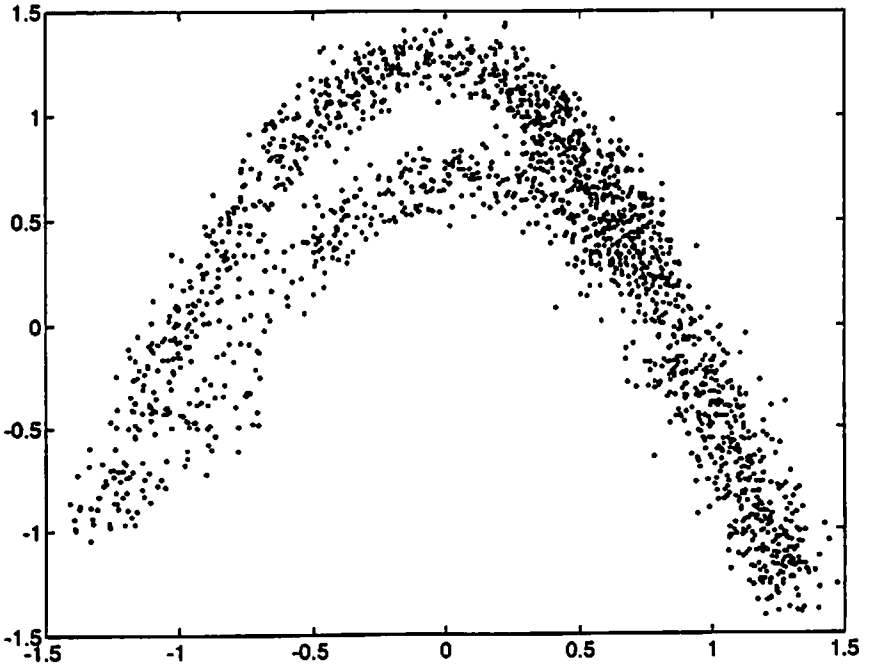

Figure 2: The attractor of the Henon map embedded in noise.

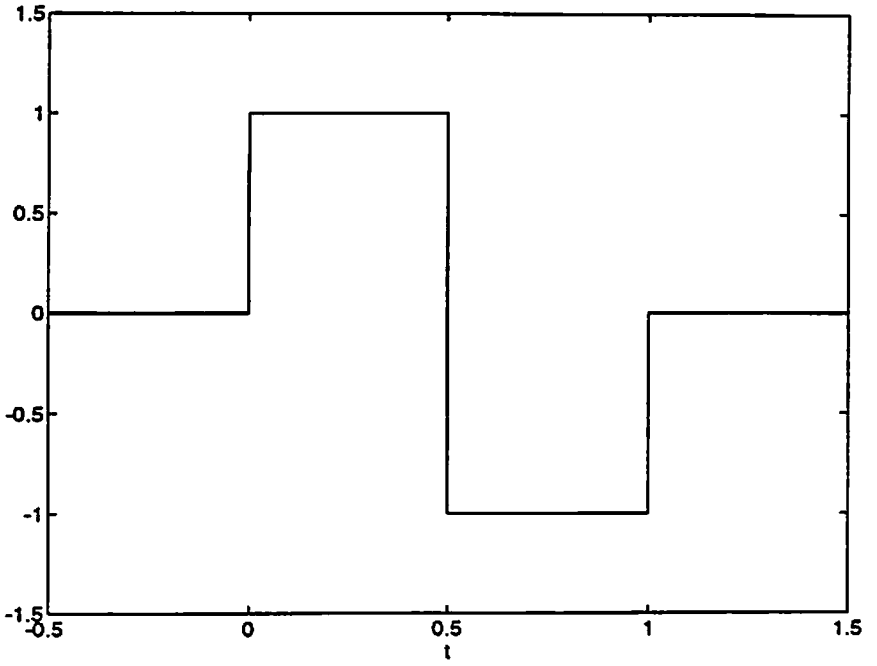

Figure 3: The Haar wavelet function

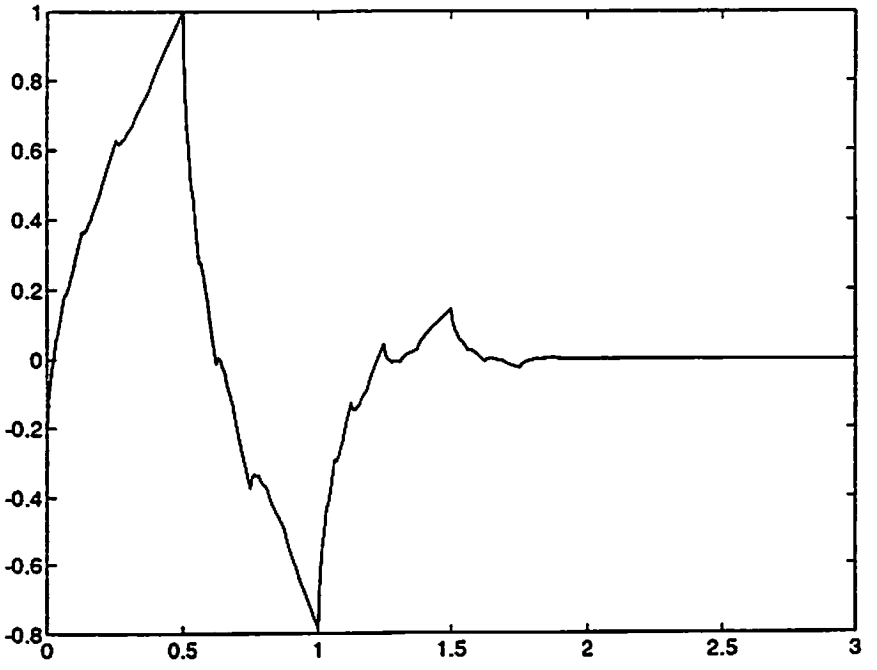

Figure 4: The Daubechies wavelet function

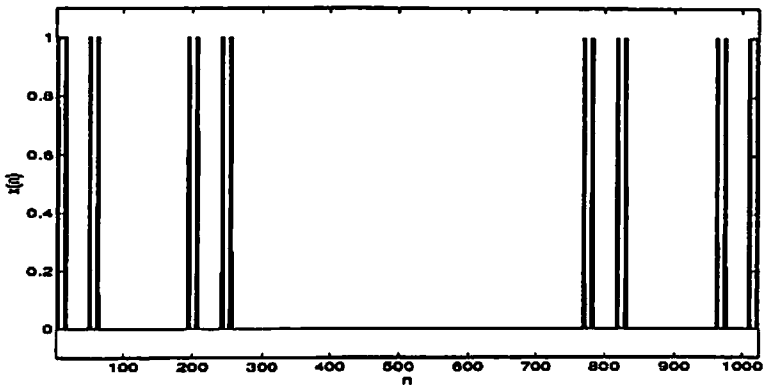

Figure 5: The self-similar cantor set

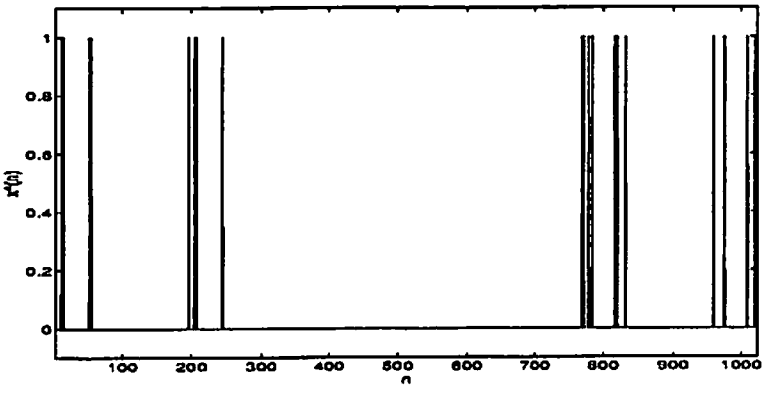

Figure 6: The self-similar cantor set randomly moved.

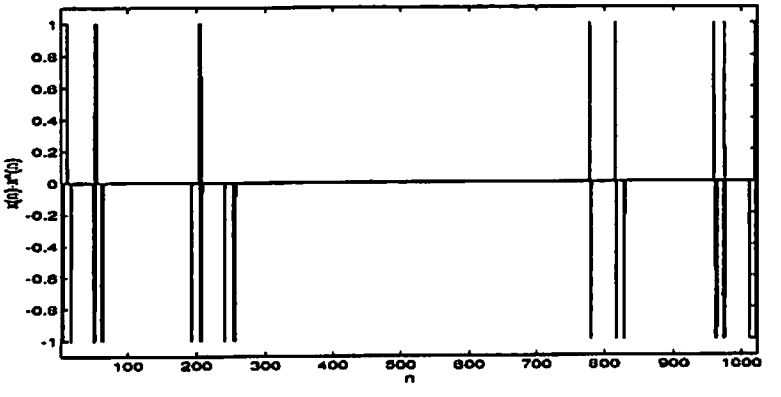

Figure 7: error

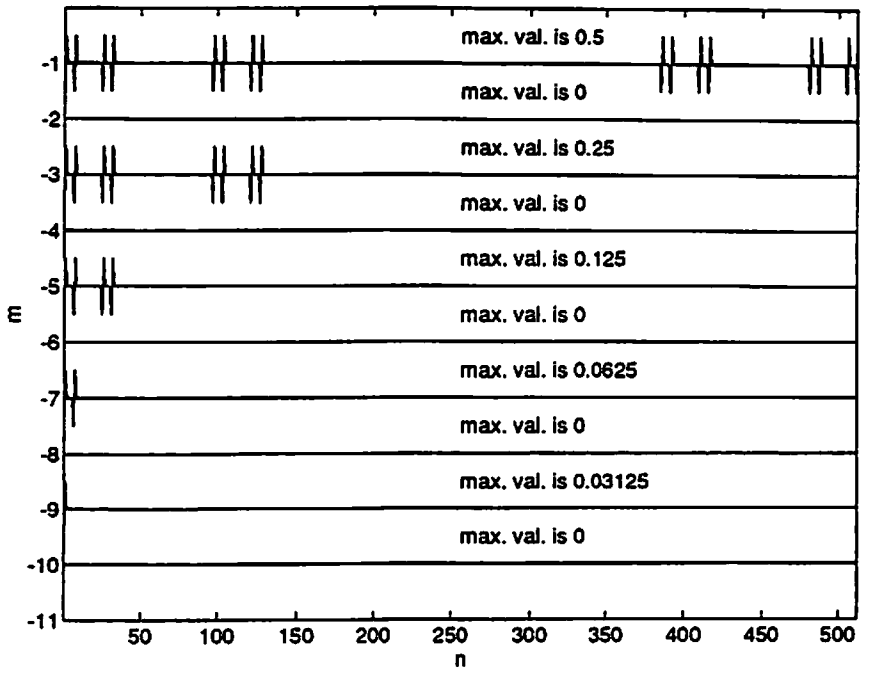

Figure 8: The wavelet transform of the self-similar cantor set

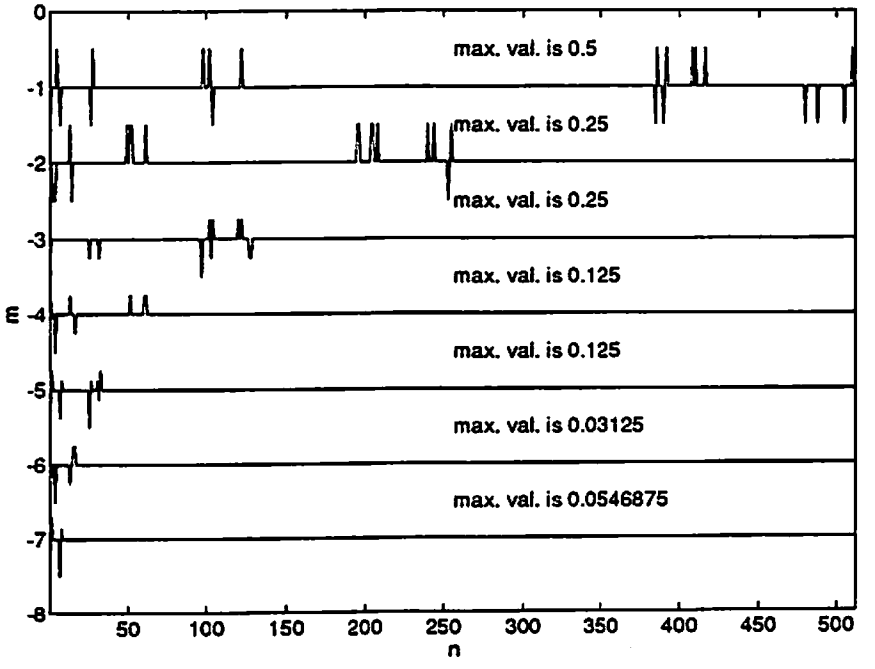

Figure 9: The wavelet transform of the self-similar cantor set randomly moved

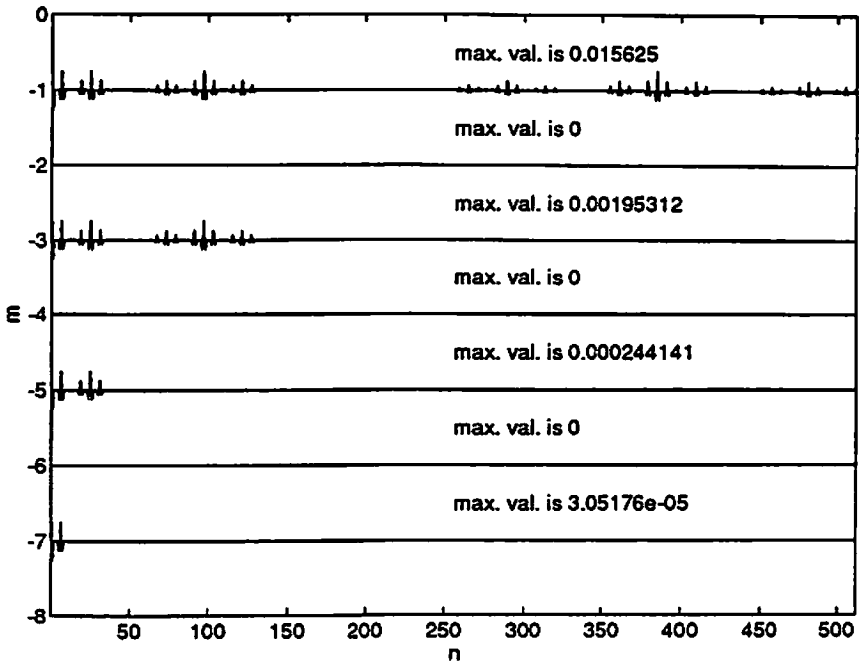

Figure 10: The correlation function of the wavelet transform of the self-similar cantor set

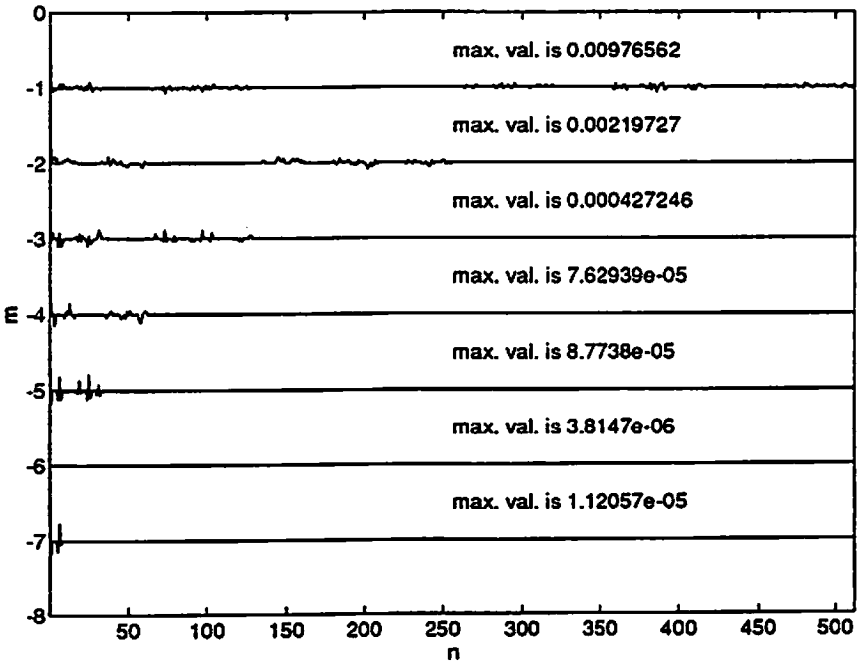

Figure 11: The correlation function of the wavelet transform of the self-similar cantor set randomly moved

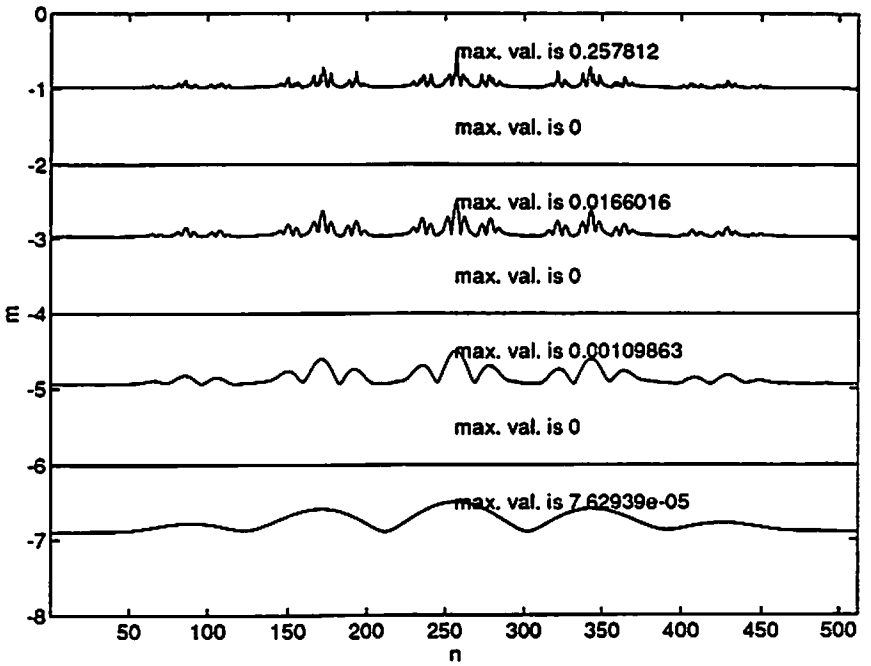

Figure 12: Power spectral density of the wavelet transform of the self-similar cantor set

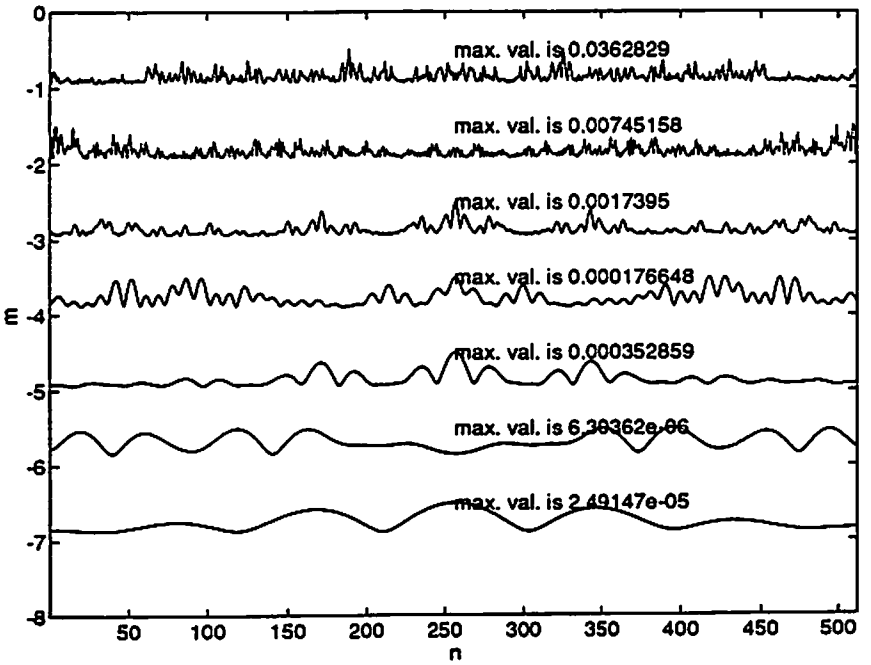

Figure 13: Power spectral density of the wavelet transform of the self-similar cantor set randomly moved

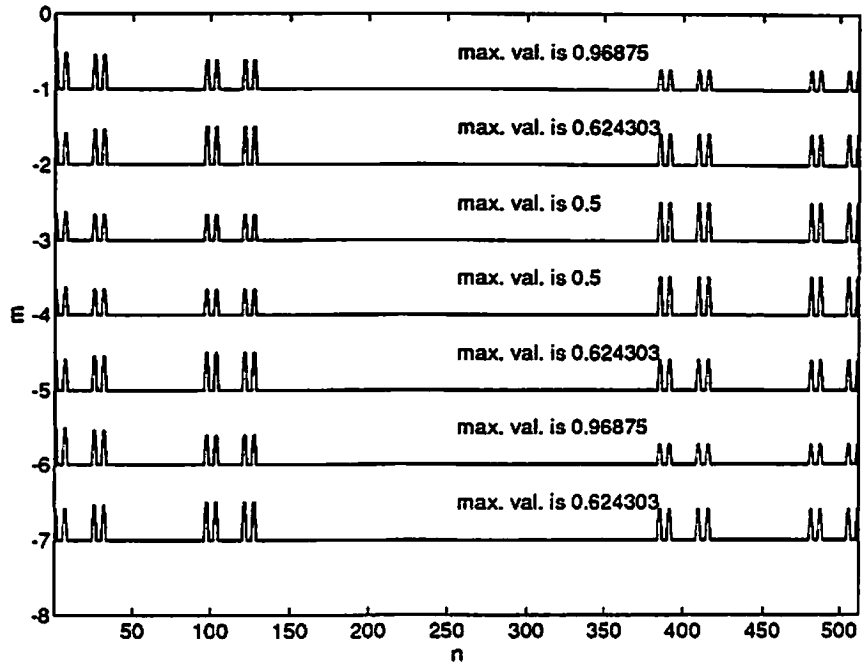

Figure 14: DFT, $\sum_m b_n^m \exp(j2\pi mk/N)$, of the wavelet transform of the self-similar cantor set.

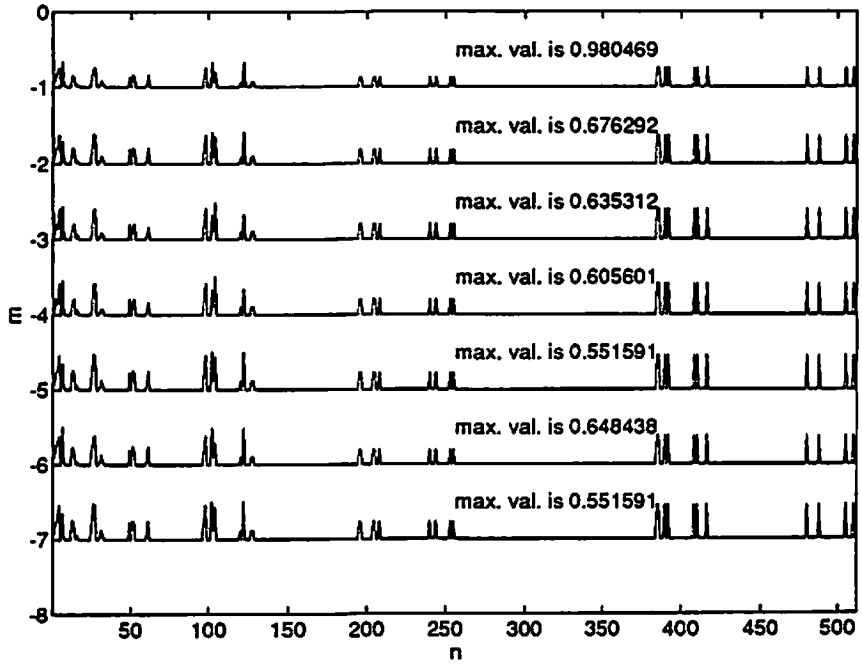

Figure 15: DFT, $\sum_m b_n^m \exp(j2\pi mk/N)$, of the wavelet transform of the self-similar cantor set randomly moved.